Bioorganic & Medicinal Chemistry 16 (2008) 6415–6422

Contents lists available at ScienceDirect

Bioorganic & Medicinal Chemistry

journal homepage: www.elsevier.com/locate/bmc

Structure–activity study of endomorphin-2 analogs with C-terminal modifications by NMR spectroscopy and molecular modeling

Chang-lin Wang [a,†], Jin-long Yao [a,†], Ye Yu [a], Xuan Shao [a], Yun Cui [a], Hong-mei Liu [a], Lu-hao Lai [a], Rui Wang [a,b,*]

[a] Key Laboratory of Preclinical Study for New Drugs of Gansu Province, Institute of Biochemistry and Molecular Biology, School of Basic Medical Science, State Key Laboratory of Applied Organic Chemistry, Lanzhou University, 222 Tianshui South Road, Lanzhou 730000, China
[b] State Key Laboratory of Chinese Medicine and Molecular Pharmacology, Department of Applied Biology and Chemical Technology, The Hong Kong Polytechnic University, Kowloon, Hong Kong, China

ARTICLE INFO

Article history:
Received 28 March 2008
Revised 30 April 2008
Accepted 1 May 2008
Available online 3 May 2008

Keywords:
Endomorphin-2
C-terminal modification
Conformation
NMR spectroscopy
Molecular modeling

ABSTRACT

Endomorphin-2 (EM-2) is a putative endogenous μ-opioid receptor ligand. To get insight into the important role of C-terminal amide group of EM-2, we investigated herein a series of EM-2 analogs by substitution of the C-terminal amide group with $-NHNH_2$, $-NHCH_3$, $-N(CH_3)_2$, $-OCH_3$, $-OCH_2CH_3$, $-OC(CH_3)_3$, and $-CH_2-OH$. Their binding affinity and bioactivity were determined and compared. Despite similar (analogs **1**, **4**, and **7**) or decreased (analogs **2**, **3**,**5**, and **6**) μ affinity in binding assays, all analogs showed low guinea pig ileum (GPI) and mouse vas deferens (MVD) potencies compared to their parent peptide. Interestingly, as for analogs **2** and **3** (a single and double N-methylation of C-terminal amide), the potency order with the K_i (μ) values was **2** > **3**; for the C-terminal esterified analogs **4**–**6**, the potency order with the K_i (μ) values was **4** > **5** > **6**. Thus, we concluded that the steric hindrance of C-terminus might play an important role in opioid receptor affinity. We further investigated the conformational properties of these analogs by 1D and 2D ^1H NMR spectroscopy and molecular modeling. Evaluating the ratios of *cis*- and *trans*-isomers, aromatic interactions, dihedral angles, and stereoscopic views of the most convergent conformers, we found that modifications at the C-terminal amide group of EM-2 affected these analog conformations markedly, therefore changed the opioid receptor affinity and in vitro bioactivity.

© 2008 Elsevier Ltd. All rights reserved.

1. Introduction

The endogenous peptide ligands for μ-opioid receptor, endomorphin-1 (Tyr-Pro-Trp-Phe-NH_2, EM-1), and endomorphin-2 (Tyr-Pro-Phe-Phe-NH_2, EM-2) were discovered in 1997 by Zadina et al.[1] Both endomorphins (EMs) exhibited the highest affinity for μ-opioid receptor and extraordinarily high selectivity relative to δ- and κ-opioid receptor systems of all known opioid substances.[1] They are also important model peptides to determine the structure–activity relationship based on their typical characteristics of backbones and aromatic side chains.[2,3]

Naturally occurring opioid peptides consist of two distinct biologically important parts, a N-terminal tri- or tetrapeptide fragment, the message sequence, and the remaining C-terminal fragment, the address sequence. Structure–activity studies showed that the message sequence needed strict requirements for a good interaction with opioid receptors. Important feathers are the presence of cationic amino group and a phenolic group in position 1, a spacer in position 2, lipophilic and aromatic residues in positions 3 and 4 for the message, and amidation at the C-terminus for the address sequence, which seems to be determinant for peptide stability.[4,5] Thus, as for EM-2, there is a strict requirement for the amino and phenolic groups of the Tyr^1, an appropriate spacer (Pro^2), and an aromatic group (Phe^3 and Phe^4).[6] According to the 'message-address' concept,[7] it is possible to consider that Tyr-Pro-Trp/Phe and Phe-NH_2 correspond to the message and address fragments, respectively.[6] These two sequences of EM-2 play an important role in ligand recognition.[6,8–11] Since the N-terminal tripeptide unit of EM-2 is considered to be the 'message' fragments, their 3D structures may be important in the formation of bioactive conformation and binding to opioid receptor, whereas, the C-terminal 'address' fragment may contribute to the stability of structure of the N-terminal tripeptide unit, resulting in the biologically active form of EM-2.[11]

A majority of bioactive peptides reveal their biological functions by C-terminal α-amidation.[12] As the deamination of such peptides leads to considerable loss of activity, the amide group may be strongly correlated with the bioactivity.[13–15] C-Terminal amidation would significantly associate with the bioactive conformation of a bioactive peptide and its interaction with a receptor. Previous

* Corresponding author. Tel.: +86 931 8912567; fax: +86 931 8911255.
E-mail address: wangrui@lzu.edu.cn (R. Wang).
† These authors contributed equally to this work.

0968-0896/$ - see front matter © 2008 Elsevier Ltd. All rights reserved.
doi:10.1016/j.bmc.2008.05.001

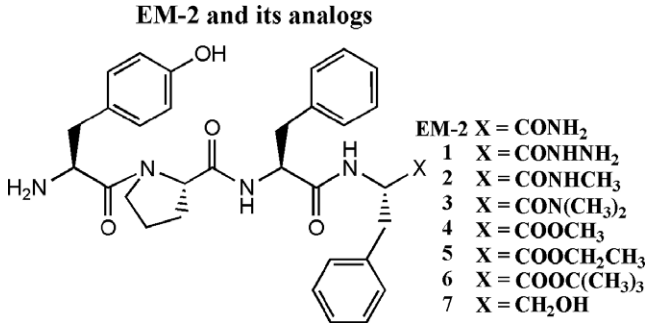

Figure 1. Schematic diagram of EM-2 and its analogs investigated in this study.

study has demonstrated that substitution of a carboxyl group for the C-terminal amide group makes the molecular conformation of EM-2 much flexible in DMSO solution. The C-terminal free acid of EM-2 leads to a considerable loss of its binding affinity and agonist activity for the μ-opioid receptor.[6,9,16] A similar decrease in activity was observed for morphiceptin and its C-terminal free acid.[17] However, the δ-opioid receptor affinity of EM-2 was increased by the substitution of a carboxyl group for the C-terminal amide group.[16] Therefore, the differentiation between the μ- and δ-opioid receptor selectivities of EM-2 is related to C-terminal region.[16] Nevertheless, the –ol derivatives of EMs, with the C-terminal amide to alcohol conversion, are high-affinity and low intrinsic efficiency agonists in the pharmacological assays in vitro.[9,10] Our previous study indicated that the C-terminal amide to alcohol conversion produced different effects on the vasodepressor activity of EM-1 and EM-2.[8] A recent review[18] reported that the replacement of the carboxamide group of EM-2 by ester (COOMe) or hydrazide ($CONHNH_2$) group produced analogs with equal or slightly improved μ-affinity compared with EM-2.

As a possible clue to the biological and structural implications of C-terminal amidation, we investigated herein the modifications of C-terminal amide group of EM-2 by substitution of the C-terminal amide group with $–NHNH_2$, $–NHCH_3$, $–N(CH_3)_2$, $–OCH_3$, $–OCH_2CH_3$, $–OC(CH_3)_3$, and $–CH_2–OH$ (Fig. 1). In the present study, we evaluated and compared the opioid receptor affinity and selectivity of these analogs by radioligand-binding assays and in vitro bioactivity assays. We further investigated the conformational properties of these analogs by 1D and 2D ^1H NMR spectroscopy and molecular modeling to reveal the conformational function of the C-terminal group of these analogs. We compared the conformations of EM-2 and its analogs generated by nuclear overhauser effect (NOE) restraints in several steric structural analysis including determining distances between two aromatic rings and the dihedral angles of the backbone and side chains.

2. Results and discussion

2.1. Radioligand binding and in vitro bioactivity assays

The affinity and selectivity of EM-2 and all its analogs (characterized in Table 1) were evaluated by radioligand binding assays using rat brain membranes. In the binding assays, [H^3]DAMGO and [H^3]DPDPE were used as μ- and δ-opioid receptor radioligands, respectively. Their binding affinities for μ- and δ-opioid receptor are summarized in Table 2. In the radioligand binding assay, analog **1** in which the C-terminal amide group of EM-2 was modified into $NHNH_2$ exhibited only slightly lower μ affinity than EM-2.[19] A single and double N-methylation of C-terminal amide of EM-2 (to give analogs **2** and **3**) produced about 3- and 33-fold greater decrease in μ affinity than EM-2, respectively. This result indicated that N-methylation of C-terminal amide was not liable to bind with μ-opioid receptor. Moreover, previous studies also reported that the EM-2 analogs, containing N-methylated amino acids, displayed reduced μ-opioid receptor affinity.[20,21] In previous study,[19] our group changed the C-terminal amide group of EM-2 into OCH_3 to give analog **4** with high affinity, similar to that of EM-2. In this study, we synthesized similar analogs **5** and **6** by changing the C-terminal amide into OCH_2CH_3 and $OC(CH_3)_3$, respectively. Interestingly, the potency order with the K_i (μ) values was **4** > **5** > **6**, but the potency order with the K_i (δ) values was **6** > **5** > **4**. Thus, we concluded that the increase in bulkiness of the esterified group might decrease the binding of an analog to μ-opioid receptor, but increase the binding to δ-opioid receptor. The –ol derivatives of EMs, with the C-terminal amide to alcohol conversion, exhibit high affinity and low intrinsic agonistic efficiency in the pharmacological assays in vitro.[9,10] Presently, our result (analog **7**) indicated similar high μ affinity (K_i (μ) = 6.34 nM).

We also evaluated the in vitro pharmacological activities using isolated guinea pig ileum (GPI) for the μ-opioid receptor and mouse vas deferens (MVD) for the δ-opioid receptor. The potencies of these analogs to inhibit an electrically evoked neurotransmitter release and the resulting muscle contractions in GPI and MVD preparations are summarized in Table 2. In the GPI assays, analogs **3** and **6** were almost devoid of activity. Furthermore, despite similar or decreased μ affinity in binding assays, analogs **1**, **2**, **4**, **5**, and **7** displayed about 4- to 14-fold lower potencies than their parent peptide. In the MVD assays, only analog **3** showed a significant decrease in MVD potency.

Table 1
Analytical data of EM-2 and its analogs

Peptide No.	Sequence	RP-HPLC (t_r)[a]	$[\alpha]_D$[b] (°)	Mp (°C)	MS $[M+H]^+$	
					Calculated	Found[c]
EM-2	Tyr-Pro-Phe-Phe-NH_2	10.365	−26	130–132	571.3	572.0
1	Tyr-Pro-Phe-Phe-$NHNH_2$	9.086	−24	142–145	586.3	587.2[d]
2	Tyr-Pro-Phe-Phe-$NHCH_3$	10.579	−27	137–139	586.3	587.2
3	Tyr-Pro-Phe-Phe-$N(CH_3)_2$	11.229	−28	121–124	599.3	600.3
4	Tyr-Pro-Phe-Phe-OCH_3	10.709	−23	108–110	586.3	587.5[d]
5	Tyr-Pro-Phe-Phe-OCH_2CH_3	12.845	−32	108–110	600.3	601.2
6	Tyr-Pro-Phe-Phe-$OC(CH_3)_3$	14.160	−27	126–128	628.3	629.3
7	Tyr-Pro-Phe-Phe-CH_2OH	11.114	−31	92–94	558.3	559.4

[a] RP-HPLC elution on a Water Delta Park C_{18} column (3.9 × 150 mm; Waters, Milford, MA). The solvents for analytical HPLC were as follows: A, 0.1% TFA in water; B, 0.1% TFA in acetonitrile. The column was eluted at a flow rate of 0.6 ml/min with a linear gradient of A/B = 80:20 to A/B = 20:80 for 30 min and A/B = 20:80 to A/B = 80:20 for 5 min.
[b] c = 0.3, MeOH (20 °C).
[c] ESI-MS.
[d] Values are cited from our group's previous report.[19]

Table 2
Opioid receptor binding affinities and in vitro pharmacological activity of EM-2 and its analogs; data are given as means ± SEM

Peptide No.	K_i (μ) [nM]	K_i (δ) [nM]	K_i (δ)/K_i (μ)	IC_{50} [nM]		GPI/MVD
				GPI	MVD	Potency ratio
EM-2[a]	8.23 ± 0.48	8360 ± 1314	1016	9.67 ± 0.84	25.8 ± 5.2	0.37
1[a]	9.35 ± 2.43	>10,000	>1070	132 ± 42.4	185 ± 79.7	0.71
2	29.17 ± 2.81	8474 ± 1558	290.5	136.2 ± 31.8	54.61 ± 23.29	2.5
3	272.7 ± 37.2	>10,000	>36.7	1810 ± 252.7	2723 ± 545	0.66
4[a]	9.07 ± 0.77	>10,000	>1102.5	42.1 ± 16.1	37.2 ± 15.0	1.1
5	14.96 ± 1.71	2940 ± 825.5	196.5	64.41 ± 6.93	63.75 ± 6.06	1.0
6	50.35 ± 7.36	247 ± 56.2	4.9	3002 ± 1264	74.12 ± 5.16	40.5
7	6.34 ± 1.35	>10,000	>1577	29.3 ± 9.0	29.17 ± 21.44	1.0

[a] Values are cited from our group's previous report.[19]

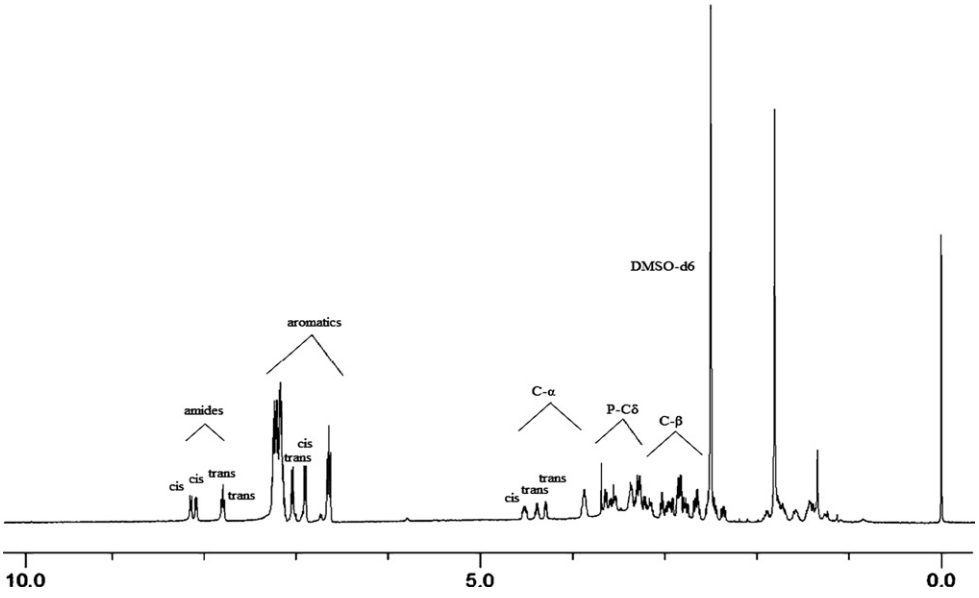

Figure 2. The assignment of ^{1}H NMR spectroscopy of [Phe^4-CH_2OH]-EM-2 (analog **7**).

2.2. NMR resonance assignments

Conformational investigations of EM-2 and its analogs were performed using standard one- and two-dimensional NMR spectroscopy in DMSO-d_6 at 298 K. The ^{1}H NMR spectra of analog **7** which had the highest μ-opioid receptor affinity exhibited two sets of conformers distinctly in the peaks of amide and aromatic protons (Fig. 2). The *cis*/*trans* isomers around the Tyr-Pro amide bond were based on the characteristic sequential NOEs observed between Tyr^1 CαH proton and Pro^2 CαH/CδH protons, and the *cis*/*trans* ratios of EM-2 and its analogs determined by the comparison of the proton peak intensities are given in Table 3. The results indicated that all the analogs had similar ratios (≈1:1) in equilibrium between *cis*- and *trans*-isomers except analog **1**. For analog **1**, the ratio of *cis*- and *trans*-isomers was 2:5. Nevertheless, it was reported that EM-2 is in equilibrium between folded and open conformers with *cis*/*trans* population ratio of 1:2 in DMSO-d_6.[6] A study with C-terminal free acid of EM-2 in zwitterionic form indicated the *cis*/*trans* population ratio of 1:2.[16] It suggests that these modifications in C-terminal amide group of EM-2 distinguished from the C-terminal free acid substitution might indicate a crucial structural requisite of C-terminus in balancing the *cis*/*trans* ratio in solution, since most of these analogs except analog **1** had higher ratios in equilibrium between *cis*- and *trans*-isomers than that in EM-2.

All proton peak assignments were performed using a combination of connectivity information via scalar coupling in TOCSY experiments and sequential NOE network cross-peaks along the peptide backbone protons. Following the protocol of structural determination in solution, the chemical shifts of all analogs are summarized in Supplementary Material. NOE cross-peak restraint determined from ROESY spectra using correlation between signal strength and interatomic distances was applied in restraint structural calculation. Based on the scalar defining the distance between two protons bonded in the same carbon atom as 1.70 Å, the NOE cross-peaks for the *cis*- and *trans*- isomers were classified as weak (1.6–5.0 Å), medium (1.6–3.6 Å), and strong (1.6–2.9 Å). All NOE cross-peaks of these EM-2 analogs were transferred for restraint data. The NOE cross-peaks and intensities of EM-2 analogs are displayed in Supplementary Material.

Table 3
The ratios[a] of *cis*- and *trans*-isomers of EM-2 and its analogs

No.	Peptide	*cis*:*trans*
EM-2	EM-2	1:2
1	[Phe^4-$NHNH_2$]-EM-2	2:5
2	[Phe^4-$NHCH_3$]-EM-2	5:6
3	[Phe^4-$N(CH_3)_2$]-EM-2	7:6
4	[Phe^4-OCH_3]-EM-2	1:1
5	[Phe^4-OCH_2CH_3]-EM-2	4:3
6	[Phe^4-$OC(CH_3)_3$]-EM-2	1:1
7	[Phe^4-CH_2OH]-EM-2	1:1

[a] Determined by integration of ^{1}H NMR.

2.3. Structural calculation with NOE restraints

Because of conformational flexibility, restrained molecular dynamics was applied to determine conformation in the case of peptides. We incorporated NOE restraints into theoretical conformational analysis and molecular dynamics. To keep the peptide bond preceding proline in the desired configuration (*cis* or *trans*), the onefold torsional potential with the constant −100 and 100 kcal/mol was imposed to force the *cis* or the *trans* configuration, respectively. For each analog, two sets of conformations were generated, depending on the configuration of this peptide bond. The *cis* and *trans* conformational ensembles of 10 least violated structures of analog **7** are displayed in Figure 3, with mean backbone RMSD deviations 0.79 and 0.62 Å, respectively. The stereoscopic views of the most convergent conformers that belong to the respective conformational groups are shown in Figure 4.

According to the conformational pattern of the backbone structure, all the NMR structures could be classified into two groups, one was S- and reverse S-type, the other was bow-shaped type. For analogs **2** and **3**, they had the opposite type of backbone conformation regarding the *cis* and *trans* configurations, which were S-type and bow-shaped type. The C-terminal esterified analogs **4–6**, with C-terminus substituted by $-OCH_3$, $-OCH_2CH_3$, and $-OC(CH_3)_3$, took the S- or reverse S-type backbone except analog **4**, which preferred bow-shaped backbone. As for the analog **7**, reverse S-type and bow-shaped type were preferred, compared to the S- and reverse S-type of analog **1**. Therefore, it suggested that modifications in the C-terminus of EM-2 resulted in different changes of the backbone conformation, and consequently showed the binding affinities to μ- and δ-opioid receptor distinguished considerably.

2.4. Distances between aromatic rings

With the abundance of aromatic amino acids and flexibility, EM-2 structures were supposed to be stabilized by the close packing of aromatic interactions instead of H-bonds.[22,23] If the distance of an aromatic ring pair between two centroids was less than 5.5 Å, an interaction of aromatic–aromatic was assumed to exist.[22,24] In this case, we analyzed the conformations of aromatic side chains and summarized the average distances of all analogs between the centroids of aromatic rings (Table 4).

As the shorter distances indicate closer aromatic–aromatic interactions, these isomers of analogs may exhibit more folded structures compared with other ones. It is noted that the two most percentage of aromatic interactions occurred in Phe^3-Phe^4 and Tyr^1-Phe^4 of *trans*-isomer of analogs **2** and **4**, respectively. Therefore, the average distances were shorter related to other analogs. Since few aromatic interactions were observed, the extended conformations were assumed to mainly exist in DMSO solution. For all the analogs, only the *trans*-isomer of analog **4** had the shortest distances between the aromatic side chains, which may be responsible for the bow-shaped folded backbone structure.

2.5. The torsions of backbone conformation and side-chain disposition

The conformational requirements of all the peptides were determined by the conformational constraint of the peptide backbone template (ϕ and ψ angles) and topographical constraint (χ^1 and χ^2) of the side chains. As seen in Table 5, the various C-terminus modifications resulted in different spatial orientations of Tyr^1, Phe^3, and Phe^4 in *cis*- and *trans*-isomers. Notably, the third and fourth phenyl rings were forced to point in nearly the opposite direction in the *trans*-isomers of analog **4** ($\chi_3^1 = -163°$ and $\chi_4^1 = -150°$) relative to analogs **5** ($\chi_3^1 = 100°$; $\chi_4^1 = 169°$) and **6** (χ_3^1=66, $\chi_4^1 = 101°$). Interestingly, for *cis*-isomers of these analogs, the situations were the same. Therefore, the substitution groups of C-terminus with $-OCH_3$, $-OCH_2CH_3$, and $-OC(CH_3)_3$ determined the spatial orientation of phenyl rings in the fourth position to some extent. In accordance with the best binding affinity to μ-opioid receptor, the $-OCH_3$ substituted group had the bow-shaped backbone conformation and different spatial orientation, both distinguished from the latter two substitutions ($-OCH_2CH_3$ and $-OC(CH_3)_3$). Therefore, we concluded that the modification in C-terminus of EM-2, influenced the backbone conformation and side-chain disposition of the fourth residue, and consequently changed the binding affinity to the μ- and δ-opioid receptor, respectively.

3. Conclusion

In the present study, to get insight into the important role of C-terminal amide group of EM-2, we investigated a series of EM-2 analogs by substitution of the C-terminal amide group with

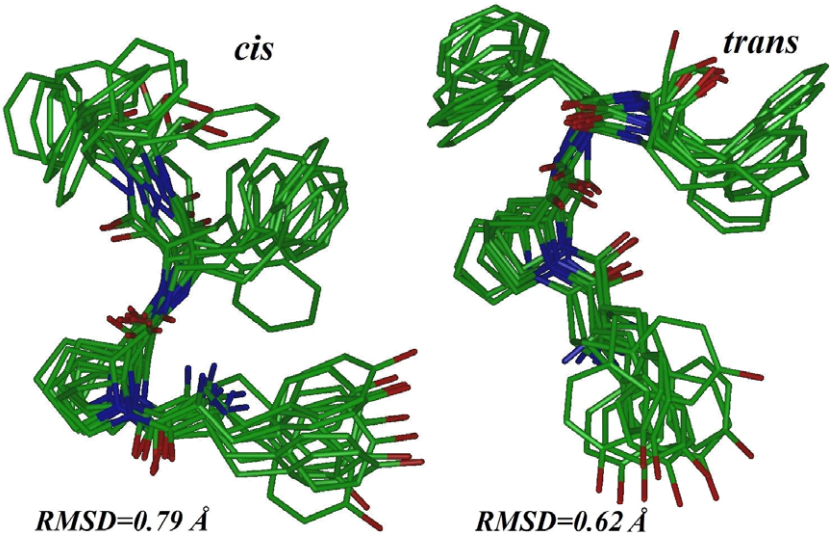

Figure 3. Ensemble of the 10 most convergent and least violated structures of the family of *cis*- and *trans*-[Phe^4-CH_2OH]-EM-2 (analog 7) determined by DG calculations and molecular dynamics with NOE distance restraints. The mean backbone RMSD of conformational clusters was labeled.

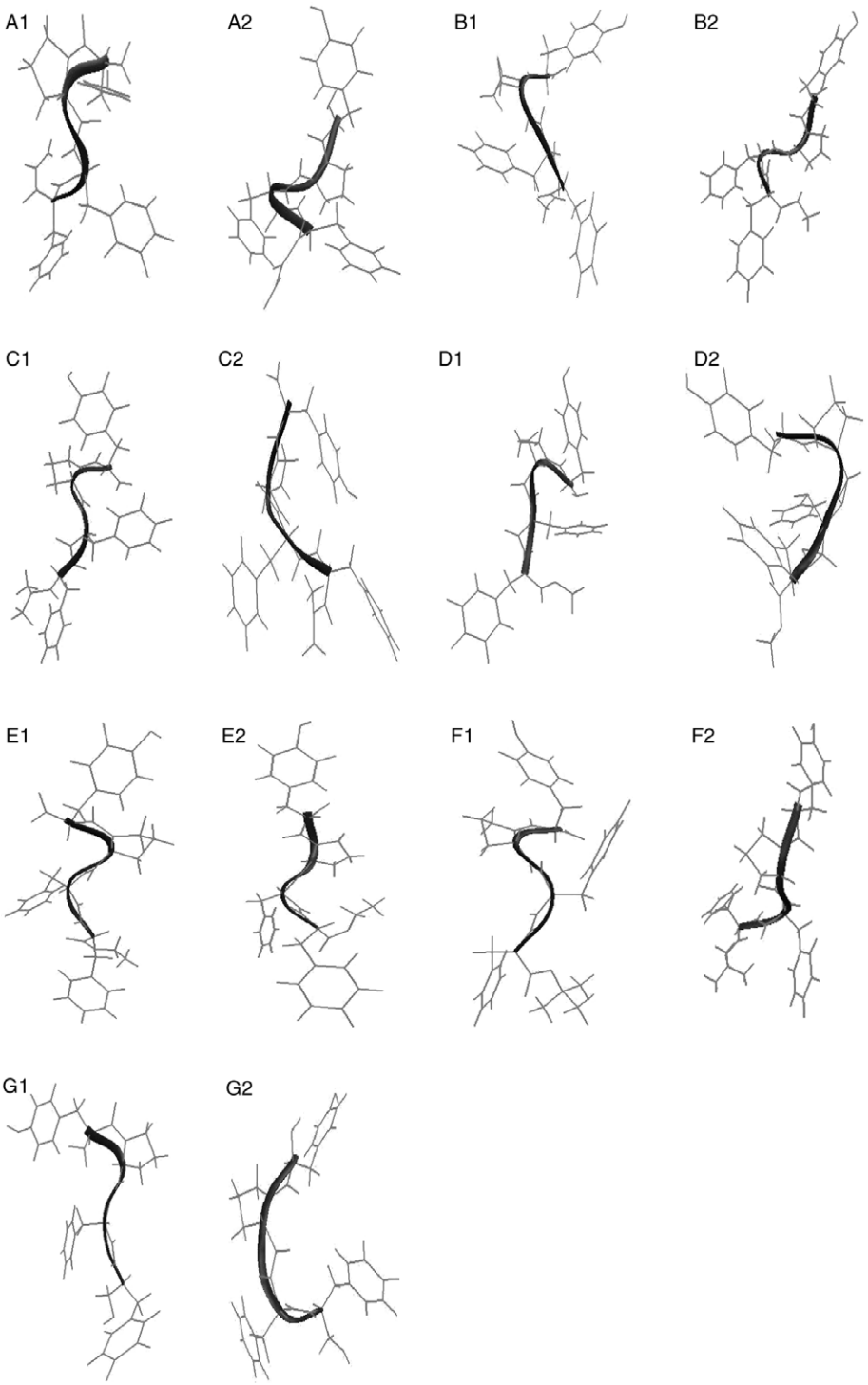

Figure 4. Stereoscopic views of the most convergent and least violated structure of the *cis*-[Phe^4-$NHNH_2$]-EM-2 (A1), *trans*-[Phe^4-$NHNH_2$]-EM-2 (A2), *cis*-[Phe^4-$NHCH_3$]-EM-2 (B1), *trans*-[Phe^4-$NHCH_3$]-EM-2 (B2), *cis*-[Phe^4-$N(CH_3)_2$]-EM-2 (C1), *trans*-[Phe^4-$N(CH_3)_2$]-EM-2 (C2), *cis*-[Phe^4-OCH_3]-EM-2 (D1), *trans*-[Phe^4-OCH_3]-EM-2 (D2), *cis*-[Phe^4-OCH_2CH_3]-EM-2 (E1), *trans*-[Phe^4-OCH_2CH_3]-EM-2 (E2), *cis*-[Phe^4-$OC(CH_3)_3$]-EM-2 (F1), *trans*-[Phe^4-$OC(CH_3)_3$]-EM-2 (F2), *cis*-[Phe^4-CH_2OH]-EM-2 (G1), and *trans*-[Phe^4-CH_2OH]-EM-2 (G2). The backbone and side-chain are represented by the thick and thin lines, respectively.

$-NHNH_2$, $-NHCH_3$, $-N(CH_3)_2$, $-OCH_3$, $-OCH_2CH_3$, $-OC(CH_3)_3$, and $-CH_2-OH$. These analogs exhibited similar or reduced μ-opioid affinity in binding assays and showed low GPI and MVD potencies. The N-methylation of C-terminal amide of EM-2 was not liable to bind with μ-opioid receptor since a single and double N-methylation of C-terminus decreased in μ affinity. In addition, the increase in bulkiness of the esterified group might decrease the binding of an analog to μ-opioid receptor. Thus, the steric hindrance of C-terminus may play an important role in opioid receptor affinity. We further investigated the conformational properties of these analogs by 1D and 2D ^{1}H NMR spectroscopy and molecular modeling. Evaluating the ratios of *cis*- and *trans*-isomers, aromatic interactions, dihedral angles, and stereoscopic views of the most convergent conformers, we found that modification at the C-terminal amide

Table 4
Average distance (Å) between the centroids of aromatic rings in EM-2 analog clusters of 100 conformations

Peptides	Tyr^1-Phe^3	Tyr^1-Phe^4	Phe^3-Phe^4
cis-EM-2[a]	7.11(11)[b]	9.52(8)	7.82(0)
trans-EM-2	8.54(7)	9.44(4)	7.69(2)
cis-[Phe^4-$NHNH_2$]-EM-2 (**1**)	7.54(0)	10.86(0)	8.42(1)
trans-[Phe^4-$NHNH_2$]-EM-2 (**1**)	11.33(0)	10.69(0)	8.73(0)
cis-[Phe^4-$NHCH_3$]-EM-2 (**2**)	8.06(2)	8.69(1)	7.32(11)
trans-[Phe^4-$NHCH_3$]-EM-2 (**2**)	11.57(0)	11.16(0)	6.38(30)
cis-[Phe^4-$N(CH_3)_2$]-EM-2 (**3**)	7.04(12)	12.91(0)	9.11(0)
trans-[Phe^4-$N(CH_3)_2$]-EM-2 (**3**)	10.14(0)	9.84(0)	9.01(0)
cis-[Phe^4-OCH_3]-EM-2 (**4**)	6.51(7)	11.89(0)	9.33(0)
trans-[Phe^4-OCH_3]-EM-2 (**4**)	7.53(9)	5.92(30)	5.85(9)
cis-[Phe^4-OCH_2CH_3]-EM-2 (**5**)	9.31(1)	12.75(0)	8.67(0)
trans-[Phe^4-OCH_2CH_3]-EM-2 (**5**)	9.90(1)	13.66(0)	9.09(0)
cis-[Phe^4-$OC(CH_3)_3$]-EM-2 (**6**)	8.58(0)	12.20(0)	8.86(1)
trans-[Phe^4-$OC(CH_3)_3$]-EM-2 (**6**)	10.64(1)	11.47(0)	8.36(1)
cis-[Phe^4-CH_2OH]-EM-2 (**7**)	7.87(11)	11.45(0)	8.15(9)
trans-[Phe^4-CH_2OH]-EM-2 (**7**)	8.25(11)	10.38(1)	7.30(1)

[a] Data from Ref. 23.
[b] The percentage of distance within 5.5 Å is given in bracket.

group of EM-2 affected these analog conformations markedly, therefore changed the opioid receptor affinity and in vitro bioactivity. On the basis of our present study, these results gave the evidence that the C-terminal residue was essential for high-affinity binding of EMs to μ-opioid receptor and for the development of suitable μ-opioid therapeutics.

4. Experimental

4.1. Peptide synthesis

4.1.1. Synthesis of HCl·Phe-OCH_3

H-Phe-OH (10 mmol) was dissolved into absolute methanol (40 ml), then distilled $SOCl_2$ (10 ml) was dropwise added to the solution under ice-salt bath below −20 °C. The reaction mixture was stirred at room temperature for 1 h, and refluxed for 4 h. Solvents were then evaporated in vacuo. The residue was crystallized from abundant ice-cold petroleum ether (PE). The product was washed with ether for several times to obtain the white powder.

4.1.2. General procedure for the synthesis of Z-Phe-OCH_2CH_3/Z-Phe-$OC(CH_3)_3$

Absolute ethanol (0.7 ml) or tertiary butyl alcohol (1.2 ml) was added to distilled CH_2Cl_2 (8 ml) containing Z-Phe-OH (2 mmol) and DMAP (0.8 mmol) at 0 °C. After 5 min, a solution of DCC (2.4 mmol) in distilled CH_2Cl_2 (4 ml) was added to the mixture. The mixture was stirred for 30 min at 0 °C and at room temperature overnight. DCU was then removed by filtration. Solvents were then evaporated in vacuo. After removal of the solvents, the residue was extracted with EtOAc and washed with 5% citric acid, saturated $NaHCO_3$, and saturated NaCl. The organic phase was dried over Na_2SO_4, and evaporated in vacuo. Crude products were purified by silica gel column chromatography (eluent: PE/EtOAc 2:1) with a yield of 81% for Z-Phe-OCH_2CH_3 and 78% for Z-Phe-$OC(CH_3)_3$.

4.1.3. General procedure for the synthesis of Boc-Phe-$NHCH_3$/Boc-Phe-$N(CH_3)_2$

To a stirred suspension of Boc-Phe-OH (2 mmol) and HOSu (2.4 mmol) in anhydrous THF (10 ml), DCC (2.4 mmol) in THF was added to the solution at 0 °C. The reaction mixture was stirred for 30 min at 0 °C and 6 h at room temperature. After DCU was removed by filtration, the remaining solution was added to methylamine alcoholic solution (4 ml) or 30% dimethylamine aqueous solution (8 ml) at 0 °C. The mixture was stirred for 30 min at 0 °C and at room temperature overnight. Solvents were then evaporated in vacuo. After removal of the solvents, the residue was extracted with EtOAc and washed with 5% citric acid, saturated $NaHCO_3$, and saturated NaCl. The organic phase was dried over Na_2SO_4, and evaporated in vacuo. The residue was dissolved in EtOH (10 ml), and distilled H_2O (150 ml) was added to the solution at 4 °C to obtain a precipitate, which was collected by filtration and dried in vacuo. The yield of Boc-Phe-$NHCH_3$ is 96%, and the yield of Boc-Phe-$N(CH_3)_2$ is 77%.

4.1.4. Synthesis of Boc-Phe-Phe-OCH_3

Boc-Phe-OH (5 mmol) was dissolved into anhydrous THF (25 ml), then NMM 0.56 ml (5 mmol) and IBCF 0.67 ml (5 mmol) were dropwise added to the solution under ice-salt bath below −20 °C. The reaction mixture was stirred at −20 °C for 5 min to form mixed acid anhydride. HCl·Phe-OCH_3 (5 mmol) was dissolved into distilled DMF (10 ml), then NMM 0.56 ml (5 mmol) was added to neutralize. After that the solution was added to the mixed acid anhydride and the reaction mixture stirred at room temperature overnight. Solvents were then evaporated in vacuo. After removal of the solvents, the residue was extracted with EtOAc and washed with 5% citric acid, saturated $NaHCO_3$, and saturated NaCl. The organic phase was dried over Na_2SO_4, and evaporated in vacuo. The residue was crystallized from EtOAc/PE with a yield of 96%.

Table 5
Torsion angles of DG-calculated structures of EM-2 analogs used in the structure comparison[a]

Peptide	Tyr^1		Pro^2		Phe^3			Phe^4		
	Ψ_1	χ_1^1	Φ_2	Ψ_2	Φ_3	Ψ_3	χ_3^1	Φ_4	Ψ_4	χ_4^1
cis-[Phe^4-$NHNH_2$]-EM-2 (**1**)	−79	−121	2	−142	−123	−61	−113	−137	78	−167
trans-[Phe^4-$NHNH_2$]-EM-2 (**1**)	162	38	−54	173	−86	50	49	−66	98	−108
cis-[Phe^4-$NHCH_3$]-EM-2 (**2**)	180	−62	−71	−180	180	−180	−58	180	180	−58
trans-[Phe^4-$NHCH_3$]-EM-2 (**2**)	82	−81	−49	106	−24	93	159	54	68	175
cis-[Phe^4-$N(CH_3)_2$]-EM-2 (**3**)	114	−165	−51	152	−85	165	−76	−85	145	138
trans-[Phe^4-$N(CH_3)_2$]-EM-2 (**3**)	139	−165	−87	91	−3	93	65	−20	89	163
cis-[Phe^4-OCH_3]-EM-2 (**4**)	142	147	−90	58	8	−150	−104	178	—	−131
trans-[Phe^4-OCH_3]-EM-2 (**4**)	−176	−78	−120	67	159	−169	−163	−176	—	−150
cis-[Phe^4-OCH_2CH_3]-EM-2 (**5**)	164	93	−63	146	−102	99	149	−60	—	135
trans-[Phe^4-OCH_2CH_3]-EM-2 (**5**)	82	−70	−84	156	−90	135	100	−9	—	169
cis-[Phe^4-$OC(CH_3)_3$]-EM-2 (**6**)	152	94	−52	152	−107	127	3	−117	—	115
trans-[Phe^4-$OC(CH_3)_3$]-EM-2 (**6**)	81	−59	−85	114	−52	170	66	−115	—	101
cis-[Phe^4-CH_2OH]-EM-2 (**7**)	80	−79	−73	158	−127	155	87	—	—	55
trans-[Phe^4-CH_2OH]-EM-2 (**7**)	98	−44	−57	180	−14	112	84	—	—	57

[a] All angles reported in degrees.

4.1.5. General procedure for the synthesis of Z-Phe-Phe-OCH_2CH_3 /Z-Phe-Phe-$OC(CH_3)_3$

Z-Phe-OCH_2CH_3/Z-Phe-$OC(CH_3)_3$ (1 mmol) was dissolved in distilled MeOH (8 ml) containing Pd/C (80 mg) and H_2, and the reaction mixture was stirred at room temperature for 3 h. After the catalyst Pd/C was removed by filtration, the solvent was evaporated in vacuo, and the residue was dissolved in THF. The same peptide-coupling procedure as for Boc-Phe-$NHCH_3$/Boc-Phe-$N(CH_3)_2$ was employed. Crude products were purified by silica gel column chromatography (eluent: PE/EtOAc 2:1) with a yield of 81% for Z-Phe-OCH_2CH_3 and 78% for Z-Phe-$OC(CH_3)_3$.

4.1.6. General procedure for the synthesis of Boc-Phe-Phe-$NHCH_3$ /Boc-Phe-Phe-$N(CH_3)_2$

Boc-Phe-$NHCH_3$/Boc-Phe-$N(CH_3)_2$ (1 mmol) was dissolved into 12.5 M HCl/EtOAc (1:4 v/v) and stirred for 2 h at room temperature. The pH of the solution was adjusted to 10 with 2 M NaOH. The same peptide-coupling procedure as for Boc-Phe-$NHCH_3$/Boc-Phe-$N(CH_3)_2$ was employed. Crude products were purified by silica gel column chromatography (eluent: PE/EtOAc 2:1).

4.1.7. General procedure for the synthesis of Boc-Phe-Phe-NH_2/ Boc-Phe-Phe-CH_2-OH

The pH of H-Phe-NH_2·HCl/H-Phe-CH_2-OH·HCl was adjusted to 10 with 2 M NaOH. The same peptide-coupling procedure as for Boc-Phe-$NHCH_3$/Boc-Phe-$N(CH_3)_2$ was employed. Crude products were purified by silica gel column chromatography.

4.1.8. Synthesis of Z-Tyr-Pro-OH

The pH of H-Pro-OH (10.4 mmol) was adjusted to 10 with 2 M NaOH. The same peptide-coupling procedure as for Boc-Phe-$NHCH_3$/Boc-Phe-$N(CH_3)_2$ was employed. The residue was crystallized from PE/EtOAc/HOAc (60:10:1). The yield was 70.3%.

4.1.9. General procedure for the synthesis of Tyr-Pro-Phe-Phe-OCH_3/Tyr-Pro-Phe-Phe-$NHCH_3$/Tyr-Pro-Phe-Phe-$N(CH_3)_2$/Tyr-Pro-Phe-Phe-OCH_2CH_3/Tyr-Pro-Phe-Phe-$OC(CH_3)_3$/Tyr-Pro-Phe-Phe-NH_2/Tyr-Pro-Phe-Phe-CH_2-OH

Deprotection of the Boc- and Z-group of C-terminal fragments was performed with HCl/EtOAc and Pd/C, respectively. The same peptide-coupling procedure as for Boc-Phe-$NHCH_3$/Boc-Phe-$N(CH_3)_2$ was employed. The crude protected tetrapeptides were purified by silica gel column chromatography with a yield range of 40–90%. The Z-group deprotection was performed by treatment with Pd/C in MeOH containing H_2 at room temperature. After 5 h the solvent was evaporated in vacuo. The residue was easily purified by silica gel column chromatography.

4.1.10. Synthesis of Tyr-Pro-Phe-Phe-$NHNH_2$

Z-Tyr-Pro-Phe-Phe-OCH_3 (1.6 mmol) was dissolved into 5 ml of absolute methanol, then H_2N–NH_2·H_2O (0.6 ml) was dropwise added to the solution. The mixture was stirred for 48 h at room temperature until the precipitate was seen in the solution. Methanol was evaporated in vacuo. The remainingss mixture was deposited for 24 h. Then it was extracted with EtOAc. The extract was washed with saturated NaCl to get the product with a yield of 85%. The Z-group deprotection was performed by treatment with Pd/C in MeOH containing H_2 at room temperature. After 5 h the solvent was evaporated in vacuo. The residue was easily purified by silica gel column chromatography.

4.2. Radioligand binding assays

Membranes were prepared from Wistar rat brain (without cerebellum) according to the literature methods.[25,26] All binding experiments were performed in 50 mM Tris–HCl buffer, pH 7.4, at a final volume of 0.5 ml containing 300–500 μg/ml protein[27] (protein concentration was determined by the method of Bradford[28]). In competition experiments, the following conditions were used for incubations: [^{3}H]DAMGO (0.5 nM), 1 h; and [^{3}H]DPDPE (1 nM), 3 h.[29] At first, [^{3}H]DAMGO or [^{3}H]DPDPE was added to membrane protein suspension, then peptide samples of different concentrations were rapidly added to separate suspension. Incubations were started by the rapid addition of peptide samples to membrane suspension in a rotating incubator at 25 °C and terminated by rapid vacuum filtration though GF/C filters using cell harvester. The filters were washed thrice with 6 ml ice-cold buffer and then dried for 1 h at 80 °C. The radioactivity was measured by a Wallac Microbeta 1450 Trilux scintillation counter (GE Healthcare) after 12 h of incubation in the scintillation cocktail. The extent of nonspecific binding was determined in the presence of 10 μM naloxone. All experiments were carried out in duplicate assays and repeated at least three times. Affinity constants (K_i) were determined as described earlier.[30]

4.3. In vitro bioactivity assays

In vitro opioid activities of peptides were tested in the GPI and MVD bioassays as reported elsewhere.[31] The GPI and MVD tissues were mounted in a 10-ml bath that contained aerated (95% O_2, 5% CO_2) Krebs–Henseleit solution at 37 and 36°C, respectively. Twitch contractions were evoked by rectangular pulses with the following parameters: 0.1-Hz, 50-V, 0.5-ms pulse width for GPI assay; pairs (100-ms pulse distance) of rectangular impulses (1-ms pulse width, 9 V/cm, i.e., supramaximal intensity) were repeated by 10 s for MVD assays. Isometric responses were recorded using a train gauge transducer linked to a recorder system (model BL-420 F, Taimeng Technology and Market Corporation of Chengdu, China). Dose–response curves were constructed, and IC_{50} values (concentration causing a 50% reduction of the electrically induced twitches) were calculated graphically. The values are arithmetic means of five to eight measurements.

4.4. NMR experiments

Freeze–dried peptide samples were dissolved in dimethylsulfoxide-d_6 (DMSO-d_6) (99.9% isotopic purity; Cambridge Isotope Laboratories, Andover, MA) at a concentration of 1–5 mg/500 μL. All 2D experiments were performed at 500 MHz on a Varian INOVA NMR spectrometer with a constant temperature at 298 K. The homonuclear correlation spectra, COSY, TOCSY, and ROESY were obtained using standard pulse programs. The mixing times of 80 and 300 ms were used for TOCSY and ROESY spectra, respectively.

The 2D NMR matrixes were created and analyzed using the FELIX 2004 computer program (Biosym Technologies Inc., San Diego, VA). Each two-dimensional spectrum was acquired 1024 × 1024 data matrix complex points in $t1$ and $t2$. The assignments of chemical shifts were carried out using standard protein database and custom unusual amino acid database built artificially. NOE cross-peak restraints determined from ROESY spectra using correlation between signal strength and interatomic distance were applied in restraint structural calculation by the criteria of 1.70 Å between two Cβ protons.

4.5. Computational molecular modeling

All the molecular modeling calculations were performed on an Origin 2000 workstation running the Irix 6.5 operation system (Silicon Graphics Inc., Mountain View, CA, USA). The initial random molecular structures were built for two isomers with ω torsion angles of Tyr^1-Pro^2 bond in allowance of 0° ± 10° and 180° ± 10°, respectively. Then energy minimizations with the CVFF force field (Accelrys Inc.) were carried out on Discover 98 module in the

Insight II 2000 package (Accelrys Inc.). The resulting coordinates were applied in the generation of the distance-bound matrices. Calculating by the standard protocol of the Distance Geometry (DG) II package in NMR-Refine module of Insight II 2000 with NOE restraint files exported from Felix2004. First, triangle-bound smoothing was used to check out the correction of molecular structure by minimization. The force constant used for distance restraints was 50.0 kcal/mol Å^2. Second, the structures were used to generate in four dimensions, then reduced to three dimensions with the EMBED algorithm.[32] Third, the assembly was optimized with a simulated annealing (SA) step[33] maintaining the distance constraints according to the standard protocol of the DG II package. One hundred structural ensembles were generated for every system.

In order to investigate the effect of solvents on the peptide conformations, the representative conformers generated by the above SA calculations were further subjected to molecular dynamics-simulated annealing (MD-SA) using the Discover program. The simulation was performed on the molecule in a 30 Å TIP3 water-box with the CVFF force field. The energy of the system was minimized and SA simulation was then performed, heating stepwise to a final temperature of 600 K. Gradual temperature reduction to 300 K, 20 ps equilibration, and a 10 ps production period followed. Restrained MD simulations covering 100 ps were carried out, in which the energy term for distance restraint was treated in the same way as the SA calculation. For each DG structure, MD simulation consisted of 10 ps at 300 K, time step 1.0 fs, temperature relaxation time 0.02 ps, and a period of update of nonbonded atom list 25 fs. On the basis of the root mean square deviation (RMSD) of backbone, each ensemble of the 10 most convergent and least violated conformations of EM-2 and its analogs was selected. Energies and pharmacophoric distances were measured from these DG/MD-SA structures.

Acknowledgments

This work was supported by grants from the National Natural Science Foundation of China (Nos. 20772052, 20621091, and 20525206), the Specialized Research Fund for the Doctoral Program in Higher Education Institutions (No. 20060730017), and the Chang Jiang Program of the Ministry of Education of China.

Supplementary data

Supplementary data associated with this article can be found, in the online version, at doi:10.1016/j.bmc.2008.05.001.

References and notes

1. Zadina, J. E.; Hackler, L.; Ge, L. J.; Kastin, A. J. *Nature* **1997**, *386*, 499.
2. Szatmári, I.; Biyashev, D.; Tömböly, C.; Tóth, G.; Mácsai, M.; Szabó, G.; Borsodi, A.; Lengyel, I. *Biochem. Biophys. Res. Commun.* **2001**, *284*, 771.
3. Okada, Y.; Fujita, Y.; Motoyama, T.; Tsuda, Y.; Yokoi, T.; Li, T.; Sasaki, Y.; Ambo, A.; Jinsmaa, Y.; Bryant, S. D.; Lazarus, L. H. *Bioorg. Med. Chem.* **2003**, *11*, 1983.
4. Yang, Y. R.; Chiu, T. H.; Chen, C. L. *Eur. J. Pharmacol.* **1999**, *372*, 229.
5. Gentilucci, L.; Tolomelli, A. *Curr. Top. Med. Chem.* **2004**, *4*, 105.
6. In, Y.; Minoura, K.; Ohishi, H.; Minakata, H.; Kamigauchi, M.; Sugiura, M.; Ishida, T. *J. Pept. Res.* **2001**, *58*, 399.
7. Schwyzer, R. *Ann. N.Y. Acad. Sci.* **1977**, *297*, 3.
8. Yu, Y.; Wang, C. L.; Cui, Y.; Fan, Y. Z.; Liu, J.; Shao, X.; Liu, H. M.; Wang, R. *Peptides* **2006**, *27*, 136.
9. Lengyel, I.; Orosz, G.; Biyashev, D.; Kocsis, L.; Al-Khrasani, M.; Rónai, A.; Tömböly, C.; Fürst, Z.; Tóth, G.; Borsodi, A. *Biochem. Biophys. Res. Commun.* **2002**, *290*, 153.
10. Al-Khrasani, M.; Orosz, G.; Kocsis, L.; Farkas, V.; Magyar, A.; Lengyel, I.; Benyhe, S.; Borsodi, A.; Rónai, A. Z. *Eur. J. Pharmacol.* **2001**, *421*, 61.
11. Leitgeb, B. *Chem. Biodivers.* **2007**, *4*, 2703.
12. Eipper, B. A.; Mains, R. E. *Annu. Rev. Physiol.* **1988**, *50*, 333.
13. Merkler, D. J. *Enzyme Microb. Technol.* **1994**, *16*, 450.
14. Suwan, S.; Isobe, M.; Yamashita, O.; Minakata, H.; Imai, K. *Biochem. Mol. Biol.* **1994**, *24*, 1001.
15. Imai, K.; Nomura, T.; Katsuzaki, H.; Komiya, T.; Yamashita, O. *Biosci. Biotechnol. Biochem.* **1998**, *62*, 1875.
16. In, Y.; Minoura, K.; Tomoo, K.; Sasaki, Y.; Lazarus, L. H.; Okada, Y.; Ishida, T. *FEBS J.* **2005**, *272*, 5079.
17. Chang, K. J.; Lillian, A.; Hazum, E.; Cuatrecasas, P.; Chang, J. K. *Science* **1981**, *212*, 75.
18. Janecka, A.; Staniszewska, R.; Fichna, J. *Curr. Med. Chem.* **2007**, *14*, 201.
19. Gao, Y. F.; Liu, X.; Wei, J.; Zhu, B. B.; Chen, Q.; Wang, R. *Bioorg. Med. Chem. Lett.* **2005**, *15*, 1847.
20. Kruszynski, R.; Fichna, J.; do-Rego, J. C.; Janecki, T.; Kosson, P.; Pakulska, W.; Costentin, J.; Janecka, A. *Bioorg. Med. Chem.* **2005**, *13*, 6713.
21. Janecka, A.; Kruszynski, R.; Fichna, J.; Kosson, P.; Janecki, T. *Peptides* **2006**, *27*, 131.
22. Leitgeb, B.; Tóth, G. *Eur. J. Med. Chem.* **2005**, *40*, 674.
23. Shao, X.; Gao, Y. F.; Zhu, C. J.; Liu, X. H.; Yao, J. L.; Cui, Y. X.; Wang, R. *Bioorg. Med. Chem.* **2007**, *15*, 3539.
24. Brandl, M.; Weiss, M. S.; Jabs, A.; Suhnel, J.; Hilgenfeld, R. *J. Mol. Biol.* **2001**, *307*, 357.
25. Spetea, M.; Otvös, F.; Tóth, G.; Nguyen, T. M.; Schiller, P. W.; Vogel, Z.; Borsodi, A. *Peptides* **1998**, *19*, 1091.
26. Simon, J.; Benyhe, S.; Abutidze, K.; Borsodi, A.; Szücs, M.; Tóth, G.; Wollemann, M. *J. Neurochem.* **1986**, *46*, 695.
27. Tömböly, C.; Kövér, K. E.; Péter, A.; Tourwé, D.; Biyashev, D.; Benyhe, S.; Borsodi, A.; Al-Khrasani, M.; Rónai, A. Z.; Tóth, G. *J. Med. Chem.* **2004**, *47*, 735.
28. Bradford, M. M. *Anal. Biochem.* **1976**, *72*, 248.
29. Akiyama, K.; Gee, K. W.; Mosberg, H. I.; Hruby, V. J.; Yamamura, H. I. *Proc. Natl. Acad. Sci. U.S.A.* **1985**, *82*, 2543.
30. Cheng, Y.; Prusoff, W. H. *Biochem. Pharmacol.* **1973**, *22*, 3099.
31. Shook, J. E.; Pelton, J. T.; Wire, W. S.; Hirning, L. D.; Hruby, V. J.; Burks, T. F. *J. Pharmacol. Exp. Ther.* **1987**, *240*, 772.
32. Crippen, G. M.; Havel, T. F. Distance Geometry and Molecular Conformation. Research Studies Press: Somerset, England and John Wiley: New York, 1998..
33. Nilges, M.; Clore, G. M.; Gronenborn, A. M. **1988**, *239*, p. 129.